Environmental Science Nano

Upcycling plant waste: Iron nanoparticles synthetized from Cannabis sativa enhance biomass and antioxidative properties in soybean (Glycine max)

Journal:	*Environmental Science: Nano*
Manuscript ID	EN-ART-10-2024-001018.R1
Article Type:	Paper

Upcycling plant waste: Iron nanoparticles synthetized from *Cannabis sativa* enhance biomass and antioxidative properties in soybean (*Glycine max*)

Milica Pavlicevic,[a] Shital Vaidya,[a] Terri Arsenault,[a] Anuja Bharadwaj,[a] Craig Musante,[a] Yingxue Yu,[b] Itamar Shabtai,[b] Joseph Liquori,[c] Jose A. Hernandez-Viezcas,[d] Vinka Oyanedel-Craver,[e] Jorge L Gardea-Torresdey,[d] Christian O. Dimkpa,[a] Jason C. White[a] and Nubia Zuverza-Mena*[a]

[a] – *Department of Analytical Chemistry, The Connecticut Agricultural Experiment Station, 06511 New Haven, CT, USA*

[b] – *Department of Environmental Science and Forestry, The Connecticut Agricultural Experiment Station, 06511 New Haven, CT, USA*

[c] – *Department of Plant Pathology, The Connecticut Agricultural Experiment Station, 06511 New Haven, CT, USA*

[d] - *Department of Chemistry and Biochemistry, University of El Paso, 79902 El Paso, TX, USA*

[e] – *Department of Civil and Environmental Engineering, University of Rhode Island, 02881, Kingston, RI, USA*

Corresponding Author: * Nubia Zuverza-Mena; email address: Nubia. Zuverza@ct.gov

Iron nanoparticles were phytosynthesized from biomass residues of two subspecies of *Cannabis sativa* (ssp. *sativa* and ssp. i*ndica*) and evaluated as a nanofertilizer for soybean growth. Both nanoparticles were identified as magnetite (Fe_3O_4) with a dry size smaller than 30 nm. The Fe_3O_4 nanoparticles (NPs) synthesized from ssp. *indica* (Fe NP-I) were negatively charged (- 27.2 ± 0.2 mV) with a smaller hydrodynamic diameter (164 ± 47 nm) than those from ssp. *sativa* (Fe NP-S) (+ 4.3 ± 0.1 mV; 1739 ± 146 nm). These differences were the result of variable composition of extracts from the two subspecies used for NP synthesis. Notably, *C. sativa* ssp. *sativa* contained a higher ratio of alcohols and mercaptans, while *C. sativa* ssp. *indica* contained more amines, ketones and organic acids. The dissolution of ions from the subspecies ssp. *sativa* and ssp. *indica* were 0.28 and 0.01% after 168 hours, respectively. When foliarly applied to soybean at 200 mg/L (6.25 ml per plant), Fe NPS and Fe NP-I increased content of chlorophylls by 142 % and 115 %, antioxidants by 121 % and 124 % and polyphenols by 177 % and 106 %, respectively, after 3 weeks of growth, compared to corresponding controls. However, Fe NP-S increased soybean biomass by 148 % whereas Fe NP-I had no impact on growth. These findings highlight the impact of the plant genotype on characteristics and effects of biosynthesized nanoparticles and provide novel insights for plant feedstock preferences for nanoparticle synthesis from plant waste for sustainable nano-enabled agriculture.

KEYWORDS: hemp; biomass waste upcycling; iron-based nanoparticles; green synthesis; antioxidants

Environmental Significance Statement: This work has two environmental benefits: reutilization of plant waste and prevention of ionic pollution of soil and underground water. Due to the higher bioactivity of hemp-derived nanoparticles and their lower translocation factor, "green" nanoparticles are required in lower concentration compared to commercial nanoparticles, corresponding salts and conventional micronutrient fertilizers. This ensures more efficient utilization of nano iron and less probability of toxicity and changes in soil composition.

Introduction

Plant-mediated synthesis of nanoparticles has seen increasing use in recent years, aimed at enhancing the biocompatibility of nanoparticles (NPs) with biological systems while simultaneously upcycling plant residues. However, in spite of the eco-friendly nature of the "green" synthesis of NPs, several challenges remain, including inconsistency in particle size; differential charge and oxidation state of NPs arising from variability in plant material composition and condition during synthesis; seasonality of the plant growth; potential need for further processing of feedstock material; use of high pressure and/or high temperature for synthesis; low yield; and long preparation time.[1-4] Although some of these issues are partly inherent to green technologies, and thus, will persist (e.g. seasonality of plants, changes in plant composition), others could be addressed through process optimization.

Green iron-based NPs are typically produced from leaves of medicinal, food crop,[2, 5-7], ornamental plants [8] and trees[9], as well as from the other plant tissues, including seeds, flowers and fruits.[10,11] However, relatively few studies have specifically investigated the possibility of iron or iron oxide (FexOy) nanoparticle synthesis from post-harvest plant waste. For example, López-Téllez *et al*.[12] synthesized Fe nanorods using orange peels; Venkateswarlu *et al*.[13] prepared magnetite (Fe_3O_4) NPs using plantain peels; and Abdullah *et al*.[14] used banana peels for the synthesis of iron oxide NPs. This small number of studies demonstrate that plant waste is an underutilized source of bioactive compounds to facilitate the synthesis of iron NPs. C*annabis sativa* L. exists as two subspecies: ssp. *sativa* and ssp. *indica*. Ssp. *sativa* contains less than 0.3% (m/m) per dry weight of Δ9 - tetra-hydrocannabinol (THC)) and ssp. *indica* contains more than 0.3% (m/m) per dry weight of THC. Certain bioactive compounds (such as polyphenols, terpenes, flavonoids, etc.) can act as reductive and capping agents during nanoparticle synthesis. [10-14] Although many plant species may contain such classes of compounds, the genus Cannabis is indeed recognized for its robust phytochemical profile. [10-14] Both subspecies of hemp contain a variety of the bioactive compounds, belonging to above-mentioned compound classes (terpenes, alkaloids, polyphenols, flavonoids, organic acids and carbonyl compounds).[15-21] Thus, these compounds play pivotal role in the determining size, charge and shape of the biosynthesized nanoparticles. Also, these same

compound classes exhibit anti-inflammatory, antioxidant, antiproliferative and analgesic effects.[15-21] Several metallic oxide NPs have been synthesized from hemp biomass. For example, Josiah *et al*.[16] and Sing *et al*.[21] synthesized silver and gold NPs and tested their cytotoxic and antimicrobial effects; Karmous *et al*.[19] produced copper and zinc oxide NPs that exhibited notable antifungal activity; and Korkomaz *et al*.[20] synthesized cerium oxide NPs with both antimicrobial and anticancer activity *in vitro*. Importantly, composite nanomaterials have also been prepared from hemp. For example, Yang *et al*.[22] used hemp stems to synthesize a carbon/ferrous sulfide/iron composite which was used for the removal of heavy metals from soil. Similarly, Coşkun *et al*.[23] synthesized metal ferrite composite used for dye removal from wastewater.

Iron is an essential micronutrient for plants. In addition to its positive effect on growth and yield, iron is also a cofactor, often as part of Fe-S clusters, of multiple oxidoreductases and enzymes involved in electron transport chain (such as P450s), chlorophyll synthesis, and the light reactions of photosynthesis.[24-27] Thus, iron application often increases the photosynthetic rate, total chlorophylls and antioxidant content in the plants.[24-27] Iron-based NPs exhibit many of the same effects as Fe salts, regardless if applied foliarly, as soil amendment, or formulated for seed priming. For example, Ahmed *et al*.[28] found that foliar exposure of Fe NPs increased both the mineral content and growth of goldenrod (*Solidago virgaurea* L.), while Feng *et al*.[29] reported that when wheat (*Triticum aestivum*) seeds were primed with a suspension of Fe_3O_4 NPs, plants showed higher photosynthetic rates and greater mineral and antioxidant content, but with a lower amount of malondialdehyde (indicative of reduced oxidative damage). However, given their small size and the potential to enter the cells without the use of transporters, coupled with the fact that they are less likely to dissolve in irrigation water, Fe NPs have been applied in far smaller concentrations compared to the corresponding Fe salts and are safer if ingested by animals or humans.[30,31] Importantly, at high concentrations, both Fe NPs and ionic Fe can be phytotoxic.[32] In the case of soybean, Fe phytotoxicity has been observed at soil concentrations as low as 30 mg/kg.[32]

Soybean (*Glycine max*) is the second most cultivated crop in the USA, after corn, with an acreage increase 18 % from 2002 to 2022. Worldwide soybean production is expected to reach USD 278 billion by 2031.[33] Several authors have examined the effects of commercial, chemically synthesized iron oxide NPs on soybean and found that both hematite (Fe_2O_3) and magnetite (Fe_3O_4) can increase germination rate, biomass, nitrogen fixation, protein content, chlorophyll content and yield of soybean, even under drought conditions.[34-43]

Given the current concerns over conventional agriculture's inability to meet future food security demands in a changing climate, novel strategies for agrochemical production and use are desperately needed. Thus, the aim of the current study was to synthesize, characterize, and evaluate the effects of iron oxide NPs from *Cannabis sativa* L. plant waste. Specifically, NPs generated from two different subspecies of *Cannabis* were directly compared, with the hypothesis that differences in *Cannabis*

sativa waste source will influence the properties of the resulting iron oxide NPs and thus, their effects on plants. NPs were applied foliarly to soybean at 200 mg/L and their effects on biomass, chlorophylls content, and the level of oxidative stress were compared after 3 weeks. This study adds to the growing body of literature demonstrating the unique value and impact of plant-waste derived NPs as a viable and sustainable strategy to enhance food production through nano-enabled agriculture.

EXPERIMENTAL

Chemicals, hemp subspecies, soybean seeds and soil substrate

Commercial iron (III) oxide (Fe_2O_3) NPs (alpha, 98 % purity; size: 100 nm; stock number: US3981) were purchased from US Research Nanomaterial, Inc. (Houston, Texas, USA). L-ascorbic acid and malondialdehyde salt were purchased from Sigma-Aldrich (St. Louis, Missouri, USA). Other chemicals as mentioned subsequently were purchased from Fisher Scientific (Waltham, Massachusetts, USA). Standards for inductively coupled plasma - optical emission spectrometry (ICP-OES) (Quality Control Standard 21 and Quality Control Standard 7 (in 5 % HNO_3)) were purchased from SPEX CertiPrep Inc. (Metuchen, New Jersey, USA). *Cannabis sativa* ssp. *sativa*, cultivar Wife (predominantly CBD subspecies), was grown at the Lockwood Farm (Hamden, Connecticut, USA) as described by Cahill *et al*.[38] and Arsenault *et al*.,[39] and following the harvest of inflorescences in September 2022, waste material was collected for use in NP synthesis. Sample of leaves and stems of *Cannabis sativa* ssp. *indica* (predominantly THC subspecies) were kindly provided by the Connecticut Department of Consumer Protection – Drug Control Division and Advanced Grow Labs (West Haven, Connecticut, USA). Soybean seeds (variety Karikachi) were purchased from Johnny's Selected Seeds (Fairfield, Maine, USA). Promix BX (Premier Hort Tech, Quakertown, Pennsylvania, USA) was used as a soil matrix for plant growth.

Synthesis of nanoparticles

For the preparation of plant extract, hemp leaves and stems (separately for each subspecies) were dried at 90° C overnight and the dried material was ground using a conventional kitchen blender. Two hundred mL of absolute ethanol was added to 5 g of previously ground plant material and the resulting mixture was placed on magnetic stirrer for 4h at 70° C. The mixture was left to cool for 30 min at room temperature, and solid hemp material was separated from the ethanolic extract by centrifugation (5 min, 3500 rpm). Fifteen mL of extract was separated for further analysis and the remainder was used for nanoparticle synthesis. NPs were made by combining hemp extract and 0.1M iron (II) acetate ($Fe(CH_3COO)_2$) in a 2:1 ratio (V/V). The pH of the resulting mixture was 6.17 ± 0.04. The mixture was microwaved for 4 min (in 5s intervals) and NPs were collected by centrifugation (13000 rpm, 5 min). Precipitated NPs were left to air-dry for 36h.

Characterization of extracts

Hemp extracts obtained as described above were dried for 48h at 70°C and functional groups were qualitatively analyzed using attenuated total reflectance Fourier-transform infrared spectroscopy (ATR-FTIR; Invenio spectrometer, Bruker, Billerica, MA, USA). Measurements were taken in the range 400-4000 cm^{-1}, with a resolution 4 cm^{-1} and 32 scans recorded per analysis. Spectra were baseline corrected and normalized in affiliated OPUS software.

To identify and determine differences in the composition as a function of *Cannabis* subspecies present in the plant extracts, the extracts were analyzed on two different gas chromatography-mass spectrometry (GC-MS) columns: Rxi-35 MS (15 m x 0.25 mm x 0.25 µm) and SLB R ILPAH (20m x 0.18 mm x 0.05 µm). Analyses were done using an Agilent 6890A GC system and Agilent 7890B GC with 5977A mass selective detector (MSD) (Agilent Technologies, Santa Clara, California, USA). Conditions for SLB R ILPAH column were as follows: splitless mode; injection volume – 5 µL; initial oven temperature -80° C; maximum oven temperature - 325° C; pressure – 9.3825 psi; flow – 1.5 mL/min (constant flow); hold time- 4 min. Helium was used a carrier gas. The parameters for the MSD-heater were: temperature- 250°C; transfer line temperature 250 °C; ionization: positive electron impact; Acquisition mode – scan; MS Quad – 150°C; MS Source temperature 230 °C; solvent delay – 1.0 min; low mass - 45, high mass – 400, threshold – 100; electron energy: 70 V. Measurement on Rxi-35 MS column was performed with a helium carrier gas set constant flow at 2.0 ml/min . Five µL injections were made in split mode at 250° C with a split ratio of 25:1 and a split flow of 99 mL/min. The initial oven temperature was 150° C, hold 0.1 min, ramp at 12° C/min to 325° C, hold for 2 minutes, flow for a run time of 16.68 minutes. The MSD source was set to 230° C, the MS Quad to 150° C and the transfer line to 250° C. Full scan spectra were collected from 70 to 500 AMU with a threshold of 100. For identification of individual compounds, the Wiley7NIST05 library was used with quality match of at least 80. Target area response was based on the primary ion for the spectra at a specific retention time.

Characterization of nanoparticles

All NPs involved in this study, namely: iron oxide NPs synthesized from ssp. *sativa* extract (denotated as Fe NP-S), iron oxide NPs synthesized from ssp. *indica* extract (denotated as Fe NP-I) and commercial NPs were tested in the same manner. The presence of Fe-O bonds and qualitative insights into the classes of hemp compounds capping the surface of NPs were determined using FTIR following the same procedure described for the extracts. The size of iron oxide NPs was determined by transmission electron microscopy (HT7800 TEM, Hitachi, Japan) using online Image J.JS software (v.0.5.8). Due to the low solubility of Fe NPs in water, the NPs were first dissolved in absolute ethanol (using both agitation and sonication) and then diluted 100 x with water, so that the final concentration was 0.5 mg/ml (with 0.1 % (v/v) Tween10). Nanoparticle suspensions were sonicated for 45 min at room temperature prior to measurement. The zeta potential and hydrodynamic diameter were determined using backscatter mode in a zeta sizer (Zetasizer Ultra, Malvern Pananalytical, Malvern, UK).

To determine the oxidation state of iron in iron oxide NPs, X-ray diffraction (XRD) analyses were done (Rigaku Smart Lab XRD, Rigaku, Wilmington, Massachusetts, USA). Samples were analyzed according to the manufacturer's instructions for powder samples. Parameters were as follows: tube voltage – 40 kV; tube current – 44 mA; measurement mode- Bragg-Brentano focusing; sample thickness- 2 mm; length limiting incident slit – 1 mm; mode-continuous; range: absolute; RS1 (mm) – 20; RS2 (mm) – 20.1; start (deg): 10; stop (deg): 70; step (deg): 0.05; speed duration time (degree/min): 7.

For dissolution analysis, 10 mg of the synthesized NPs were dissolved (by shaking) in 50 mL of deionized water (pH 7.0). After 1 h, 2 h, 4 h, 24 h, 48 h, 96 h and 168 h aliquots (8 mL) were taken for analysis. Prior to aliquoting, samples were shaken for 5 min and left to "settle" for 10 mins. To maintain the concentration (200 mg/L) of NPs after each aliquot collection, sample tubes were re-filled to 50 mL. The Fe concentration in the samples was determined by inductively coupled plasma – optical emission spectroscopy (ICP-OES) using Quality Control Standard 21 and Quality Control Standard 7 (iCAP Pro XP, Thermo Fisher Scientific, Waltham, Massachusetts, USA). To construct the standard curve, standards were used in concentration 0.1 mg/L, 1 mg/L and 10 mg/L.

Plant experiment design

The plant study was conducted in a greenhouse and was divided into two separate experiments. In the first experiment, NPs made from *Cannabis sativa* ssp. *sativa* were tested and this experiment consisted of four treatments: unamended control, "green" iron oxide NPs from ssp. *sativa* (Fe NP-S), commercial iron oxide NPs and $Fe(CH_3COO)_2$. In the second experiment, NPs made from *Cannabis sativa* ssp. *indica* were tested with six treatments: unamended control, "green" iron oxide NPs from ssp. *indica* (Fe NP-I), commercial iron oxide NPs, $Fe(CH_3COO)_2$, extract from *Cannabis sativa* ssp. *sativa* (marked as extract sativa), and extract from *Cannabis sativa* ssp. *indica* (marked as extract indica). All the other conditions were the same for both experiments, including soil-like media used and physical location of plant growth. Plants were germinated and grown for three weeks (25° C, 16 h light/8 h dark light regime) prior to being transplanted into bigger, experimental pots. Both NPs and salts were applied foliarly at 200 mg/L. Surfactant (Tween 10) was added (at 0.1 % (v/v) for better dispersion and retention on the leaf surface. For the control and extracts treatments ~ 6.25mL of nanoparticle or ion solution was applied per plant; deionized water was used for the controls. Each treatment consisted of 8 replicates and plants were grown in 500 ml pots with 400 mL of potting mix. The greenhouse temperature was 25° C, and plants were grown under 16h light/8h dark light regime. Effects of Fe NP-S and Fe NP-I were compared to corresponding control plants. Plants were grown for three weeks after treatment and physiological parameters were monitored weekly.

Physiological endpoints

For measurement of total chlorophylls content, the spectrometric method by Li *et al.*[44] was used. Briefly, 0.05 g of fresh, leaves were cut with scissors into 0.5 cm x 0.5 cm squares and placed into 15 mL tubes. Subsequently, the samples were extracted with 15 mL of 95 % ethanol, using a rotary shaker set to 100 rpm for 1 h at ambient temperature. Absorbance of the supernatant was measured at 649 and 665 nm (SpectraMax M2 Molecular Devices, San Jose, California, USA). The chlorophylls content was calculated using the following formulas:

$$chl\ a\left(\frac{mg}{ml}\right) = ((12.7 \times A665) - (2.69 \times A649)) \div 1000$$

$$chl\ b\left(\frac{mg}{ml}\right) = ((22.9 \times A649) - (2.69 \times A665)) \div 1000$$

$$chl\ total\ = chl\ a\ + chl\ b$$

where *Chl a* is chlorophyll a, *Chl b* is chlorophyll b, *Chl total* is total chlorophyll content, A649 and A665 are absorbances measured at 649 and 665 nm, respectively. The chlorophylls content was expressed as mg/g (fresh weight).

Antioxidant activity was measured by both the 2,2-diphenyl-1-picrylhydrazyl (DPPH) and 2,2'-azino-bis(3-ethylbenzothiazoline-6-sulfonic acid) (ABTS) assays [45,46] Briefly, for both tests, antioxidant compounds were extracted as follows: After drying overnight at 70° C, leaf samples were homogenized, and 0.125 g of each sample was extracted with 6.86 mL of 70 % ethanol(using rotary shaker, 100 rpm, room temperature, 2 h). For the DPPH assay, 100 µL of sample was combined with 1.9 mL of fresh DPPH solution (0.025 g/L DPPH in methanol), followed by incubation for 30 min in the dark, and absorbance was measured at 515 nm. The ABTS reagent was prepared 14 h earlier by mixing 5 mL of 7 mM ABTS solution (in water) with 5 mL of 2.45 mM potassium persulfate in water and the solution was kept in the dark at room temperature before use. Subsequently, the ABTS reagent was diluted with water to reach absorbance between 0.65 and 0.75 at 734 nm. For the ABTS assay, 200 µL of sample was combined with 1.8 mL of fresh ABTS solution, incubated for 15 min in the dark and absorbance was measured at 734 nm. For both assays, 6-hydroxy-2,5,7,8-tetramethylchroman-2-carboxylic acid (Trolox) was used as a standard. Antioxidant activity was expressed as Trolox equivalents (TE)/g (dry weight).

Plant cell viability was determined by the (3-(4,5-Dimethylthiazol-2-yl)-2,5-Diphenyltetrazolium Bromide (MTT) method as described by Shoemaker *et al.*[47] Briefly, leaves were dried overnight for 70°C and ground. Then 0.375 g of homogenized sample was extracted with 6.25 mL of distilled water at 100 °C for 45 min. The solution was left to cool for 30 min at ambient temperature and 500 µL was pipetted to a new vial. Then, the sample was diluted with distilled water in the ratio 1:20. The MTT assay was performed by mixing 400 µL of diluted extract, 400 µL of 1 mM ascorbic acid, 400 µL of Dulbecco's modified Eagle's medium, and 120 µL MTT solution (3 mg/mL in phosphate buffered saline), followed by incubation for 60 min at 37 °C, and absorbance measurement at 595 nm.

Determination of total polyphenolic content was performed according to a modified method by Cruz-Carrión *et al*.[48] Briefly, leaves were dried overnight at 70° C and ground. Then, 0.05 g of dried, homogenized sample was mixed with 1 mL of 80 % (v/v) methanol acidified with 0.1% (v/v) formic acid. The resulting mixture was shaken at 120 rpm for 30 min at room temperature. Plant material was separated from the extract by filtering using a 10 mL disposable syringe and Whatman disposable filters (PTFE membrane, diameter - 25 mm; pore size- 1.0 µm). Then, 200 µl of supernatant, 100 µl of Folin–Ciocalteu reagent, 200 µL of Na_2CO_3 (5 w/v % in water), and 1.5 mL of distilled water were mixed and incubated for 16 min at 50° C in dark. The absorbance was measured at 765 nm. Gallic acid was used as a standard and the total polyphenol content was expressed as gallic acid equivalents (GAE) (µg/g (dry weight)).

The method of Francesca *et al*.[49] was modified to determine malondialdehyde (MDA) content. In short, fresh leaves samples were ground using liquid nitrogen in cooled mortar and pestle on ice, and 0.2 g of ground sample was extracted with 1 mL of ice-cold 0.1% (w/v) trichloroacetic acid. The resulting mixture was then incubated for 15 min on ice and centrifuged at 13000 rpm for 10 min at 4°C. Then, 250 µL of the supernatant was combined with 1250 µL reaction solution (20% (w/v) trichloracetic acid + 0.5% (w/v) thiobarbituric acid). The mixture was incubated for 30 min at 95° C. MDA was used as standard and absorbance was measured at 532 nm. The resulting values were expressed as nmol/g (fresh weight).

The same extract was used for the determination of reduced glutathione (GSH) content and for the activity of antioxidant enzymes. In short, leaves were frozen in liquid nitrogen and 0.5 g of frozen sample was ground using cooled mortar and pestle with 6 mL of extraction buffer. The composition of the extraction buffer was the same as described in Shu *et al*.[50] (50 mM potassium phosphate buffer (pH 7.8), 0.1 mM EDTA and 0.3% (v/v) Triton X-100). The mixture was ground for 5 min on ice and centrifuged for 5 min at 10 600 x g at 4° C. The supernatant was then used for determining GSH content and the activity of catalase (CAT), peroxidase (POD) and superoxide dismutase (SOD) enzymes.

GSH concentration was determined using the method by Paesano *et al*.[51] Briefly, 500 µL of supernatant from previous step was combined with 1500 µL of test buffer [0.1 mM ethylenediaminetetraacetic acid (EDTA) and 5 mM 5,5-dithiobis (2-nitrobenzoic acid) in phosphate buffered saline] and incubated for 16 min at 30° C. GSH was used as the standard and absorbance was read at 412 nm. Values were expressed as mg/g fresh weight.

The activities of the antioxidant enzymes, namely, peroxidase, catalase, and superoxide dismutase were measured as described by Çelik *et al*.[52] For peroxidase, 100 µl of extract was combined with 750 µl of 20 mM sodium acetate buffer pH 5.0, 50 µL of 20 mM guaiacol and 100 µL of substrate (30 mM H_2O_2). Absorbance was measured at 470 nm after 0, 1, 2 and 3 min. The extinction coefficient was 26.6 mM−1 cm−1 and a unit (U) of peroxidase activity was defined as mmol H_2O_2 ml^{-1} min^{-1}. For catalase, 100 µl of supernatant was mixed with 800 µl of 0.5 M sodium phosphate buffer pH 7.0 and 100 µl of substrate (0.3 M

H_2O_2). Absorbance was then measured at 240 nm at 0, 1, 2 and 3 min. To calculate catalase units (defined as 1 mmol H_2O_2 ml−1 min−1), an extinction coefficient 39.4 mM^{-1} cm^{-1} was used. For superoxide dismutase, 100 µl of extract was added to 1.9 ml of solution containing 50 mM sodium phosphate buffer (pH 7.8), 033 mM nitro blue tetrazolium chloride (NBT), 10 mM L-methionine, 0.66 mM Na_2EDTA and 0.0033 mM riboflavin. Absorbance was then recorded at 560 nm after 0, 3, 5, and 10 min. The extinction coefficient was 39.4 mM^{-1} cm^{-1}, and SOD activity unit was defined as % of inhibition of NBT. Activities of all enzymes were expressed as U/mg fresh weight.

Measurement of iron content in plant tissues and iron content in nanoparticles

For the determination of Fe content in the plant shoot and root, samples were dried at 70°C for 24h and ground separately. Then 0.3 g of homogenized root or shoot were separately digested with 5 mL of 68% nitric acid and 1 ml of H_2O_2 (30 % v/v) for 45 min at 115° C (DigiPrep MS, SCP Science, Champlain, New York, USA). The samples were diluted to 50 mL with distilled water and Fe content was determined by ICP-OES (iCAP Pro XP, Thermo Fisher Scientific, Waltham, Massachusetts, USA) using Quality Control Standard 21 and Quality Control Standard 7. To construct the standard calibration curve, standards were used in concentration 0.1 mg/L, 1 mg/L and 10 mg/L. For measuring of Fe content in the NPs, NPs were first dissolved in 2 ml of absolute ethanol and then diluted 10-fold with deionized water and sonicated for 45 min. The ICP-OES method used to determine Fe content in NPs was the same as the one used for determination of Fe content in shoots and roots.

Statistical analysis

All analyses were done in triplicate. Prior to statistical analyses, all data were normalized by dividing each individual value with average value for corresponding control at given time point (0 days, 7 days, 14 days and 21 days). A one-way analysis of variance (ANOVA) was employed to assess differences among treatments at different time points. Differences among treatment means were analyzed by the Tukey test ($p < 0.05$). Statistical analyses were performed in SPSS software version 24 (IBM, Armonk, New York, USA).

RESULTS AND DISCUSSION

Characterization of extracts

To assess the presence of different functional groups in the hemp (*Cannabis sativa*) tissues, both extracts were analyzed using ATR-FTIR. Both extracts contained molecular bonds that indicate the presence of alcohols, aromatic compounds, carbonyl compounds, organic acids and saturated/aliphatic hydrocarbons (Figure 1, Table S1). Several of these functional groups are known to participate in the reduction of ions and mediate nanoparticle formation and aggregation.[15-21] However, the absorbances of these bonds in the two extracts were overtly different, indicating different relative abundances. Peaks in both spectra showed slight shift from values found in reference tables due to the presence of the multiple compounding and stretching, vibration or

bending of bonds in them. The extract obtained from *Cannabis sativa* ssp. *sativa* appeared to exhibit a greater presence of alcohols and aromatic compounds, whereas that from *Cannabis sativa* ssp. *indica* contained more esters and alkanes (Figure 1). Due to the differential presence of these classes of compounds, certain key properties of NPs, such as dissolution, charge and size, were expected to vary.

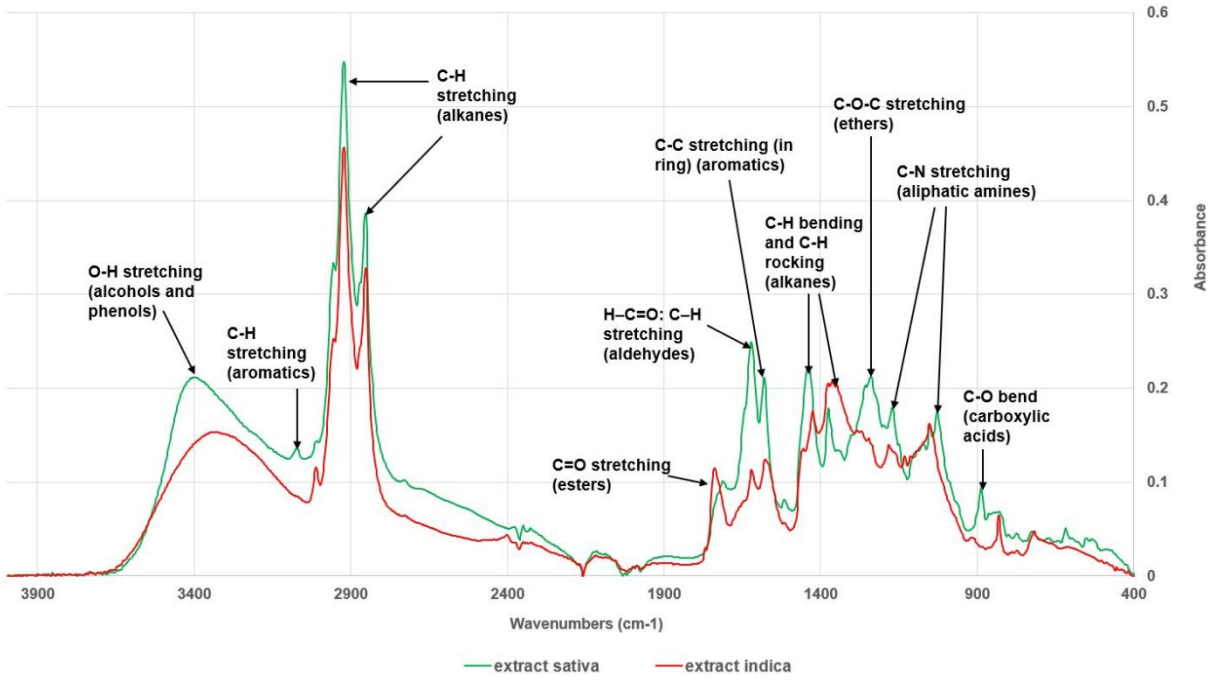

Figure 1: FTIR spectra of *Cannabis sativa* ssp. *sativa* and *Cannabis sativa* ssp. *indica* extracts

Gas chromatography mass spectrometry (GC-MS) was used to further investigate the differences in the plant extract composition between the two hemp cultivars and to elucidate which individual compounds might contribute to the observed differences in subsequent plant response. Figure 2 gives percentage of different classes of compounds present in extract from ssp. sativa and ssp. indica, whilst Table S2 lists the compounds present in both extracts, as well as those specific to each extract (i.e., compounds that do not overlap), together with their relative amounts. Only compounds identified with more than 80% certainty were included in the table. GC-MS analysis confirmed the presence of the same classes of compounds indicated by FTIR spectra; alcohols (including sterols and phenols) were the most common class detected in both extracts, followed by alkaloids (in particular, cannabinoids) and cyclic and aliphatic alkenes (Figure 2, Table S2). Other classes of compounds detected in both extracts included terpenes, organic acids, aromatic and carbonyl compounds. Therefore, compounds present in both extracts were crucial for the synthesis of NPs, but don't explain differences in size, charge and polarity between NPs synthesized from different subspecies of *Cannabis sativa*. Consistent with their ATR-FTIR spectra, *C. sativa* ssp. *sativa* contained more alcohols

(including sterols and phenols), alkanes (both acyclic and cyclic) and mercaptans, whereas *C. sativa* ssp. *indica* had a higher ratio of nitrogen (N)-containing and carbonyl compounds, as well as organic acid and esters. The relative amounts of aromatic compounds and terpenes were similar in both extracts (Figure 2, Table S2).

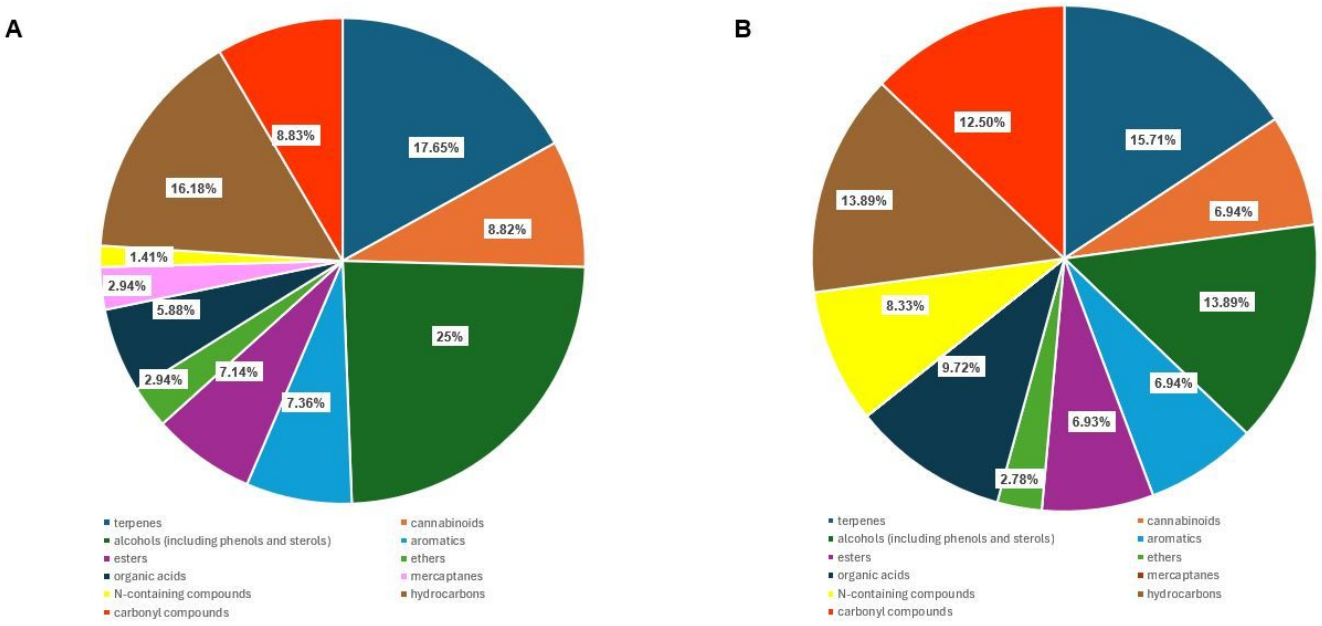

Figure 2: Percentage of specific classes of compounds present in extracts of *Cannabis sativa* ssp. *sativa* (A) and *Cannabis sativa* ssp. *indica* (B)

Characterization of nanoparticles

FTIR analysis was performed to evaluate functional groups associated with the NPs (Figure 3). In the "fingerprint region" (400-1000 nm), stretching of Fe-O bonds in the commercial Fe_2O_3 NPs showed two characteristic peaks at 428 cm^{-1} and at 513 cm^{-1}. These findings agree with the results reported by Hussain *et al*.[39] who showed peaks representative of Fe-O bond at 435 cm^{-1} and 520 cm^{-1}. However, peaks coming from the stretching of Fe-O and Fe-O-Fe bonds were shifted towards higher wavenumbers in both of NPs synthesized from ssp. *sativa* extract (Fe NP-S) and NPs synthesized from ssp. *indica* extract (Fe NP-I). For NPs synthesized using *C. sativa* ssp. *sativa,* peaks were visible at 614 cm^{-1} and 657 cm^{-1}, while for NPs synthesized using *C. sativa* ssp. *indica,* peaks were detected at 659cm^{-1} and 702cm^{-1} (Figure 2). This shift may be due to the presence of aldehydes, alkanes, amines and imines, aromatics, esters and organic acids on the NPs. The impact of residual plant molecules on the shift of Fe-O and Fe-O-Fe stretching frequency has been documented by several authors. For example, Lakshminarayanan *et al*.[41] found that Fe_2O_3 NPs synthesized from *Bauhinia tomentosa* leaf extracts showed characteristic peaks at 555 cm^{-1} and 811 cm^{-1}; Maldivoli *et al*.[42] detected a peak originating from Fe-O bond in Fe NPs synthesized from *Ageratum conyzoides* extract at 686 cm^{-1}; Aida *et al*.[5]

observed characteristic peak at 592 cm^{-1} when analyzing Fe_2O_3 NPs synthesized from hibiscus extract. The biggest differences between Fe NP-S and Fe-NP-I and the chemically synthesized commercial counterpart were seen at 1800-800 cm^{-1} (Figure 3),

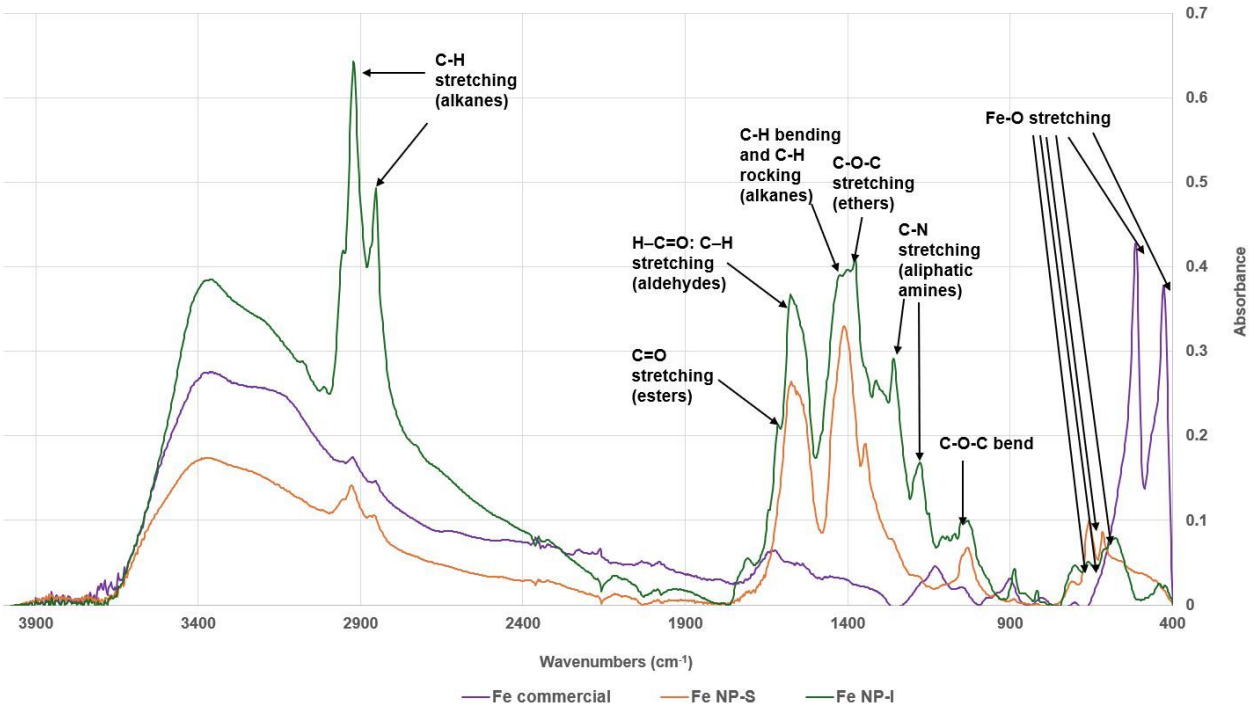

indicating that significant amounts of N-containing compounds, carbonyl compounds, ethers and alkanes were associated with the biosynthesized NPs.

Figure 3. FTIR spectra of commercially available chemically synthesized Fe_2O_3 nanoparticles (Fe commercial), iron nanoparticles synthesized from *Cannabis sativa* ssp. *sativa* (Fe NP-S); and iron nanoparticles synthesized from *Cannabis sativa* ssp. *indica* (Fe NP-I).

The size of the NPsalso varied as a function of hemp subspecies (Figure S1). The average size of nanoparticles (determined by TEM) synthesized from *C. sativa* ssp. *sativa* was 25.4 ± 3.5 nm, while the average size of nanoparticles synthesized from ssp. *indica* was 9.7 ± 2.1 nm. In the literature, reported sizes of Fe NPs synthesized from plant extracts vary from 4 nm to 200 nm.[3,4] Such a broad size range is due mainly to the variability in plant composition, aggregation and synthesis conditions. Both NPs were roughly spherical (Figure S1). Although Kiwamulo et al.[6] reported that the shape of Fe NP depends on size, spherical shape of NPs was observed by multiple authors in the size range of 8.5-86.0 nm.[5-9,14,41,43]

Identified peaks on the X-ray diffraction (XRD) spectra are shown in Figure 4. For Fe NP-S, peaks at 24.00, 24.30, 27.31 and at 51.02 degrees were identified as iron (III) oxide (DB card number 01-076-1821); peaks at 35.11 and 36.46 degrees were identified as magnetite (Fe_3O_4) (DB card number 01-080-6410); peaks at 26.55 and 32.89 degrees were identified as iron (II) oxide (DB card number 01-074-6271). For Fe NP-I peaks at 15.69, 24.15 and 26.22 were identified as iron (II) oxide (DB card number 01-074-6271); peaks at 25.25 and at 49.87 were identified as iron (III) oxide (DB card number 01-076-1821); peaks at 26.93 and 27.71 degrees were identified as magnetite (Fe_3O_4) (DB card number 01-080-6410). Aida *et al*.[5] and Abdullah *et al*.[14] reported peaks at similar values for "green" Fe NPs synthesized from hibiscus extract and banana peel extracts, respectively. It is also evident that Fe NP-I were more amorphous than Fe NP-S which likely contributed to their lower solubility (Figure S2) and adsorbtion.[53] Importantly, given that in both nanoparticles, Fe is present in both +2 and +3 oxidation states, it is likely that these materials could participate in a broad range of physiological activities in plants.

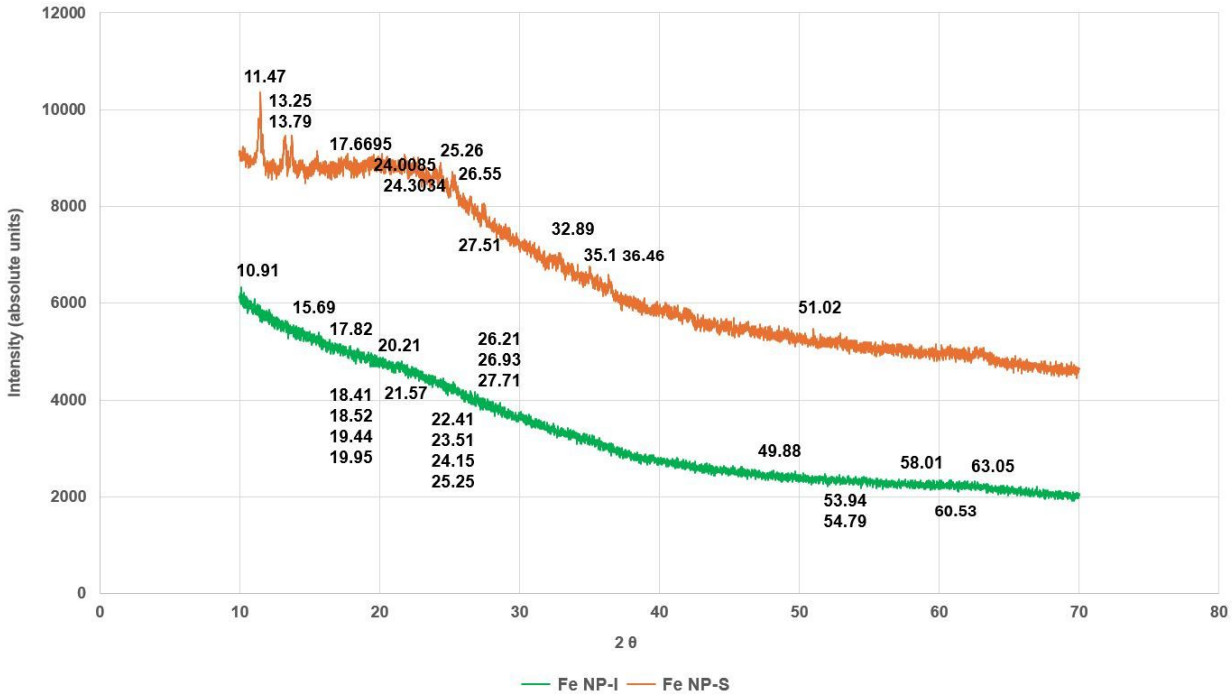

Figure 4. X-ray diffraction (XRD) spectra of iron nanoparticles. Fe NP-S -Iron nanoparticles synthesized from *Cannabis sativa* ssp. *sativa*; Fe NP-I- Iron nanoparticles synthesized from *Cannabis sativa* ssp. *indica*.

The zeta potential and hydrodynamic diameter of the nanoparticles also depended on the hemp subspecies from which they were synthesized (Table S3). Given the greater presence of organic acids in the ssp. *indica* (Figure 3, Table S2), NPs made from this extract were negatively charged, with a value of -27.2 ± 0.2 (Table S3), which indicates good stability. Given that ssp. *sativa* contained more alcohols, the greater formation of hydrogen bonds with water (which was used as a solvent) is likely, which might

explain the tendency toward aggregation, higher hydrodynamic diameter, and slightly positive charge suggesting low stability. Cao *et al*.[36] reported that smaller Fe_2O_3 NPs (4–15 nm) applied foliarly typically have greater impact on the growth of soybean. Therefore, the bioactivity of these NPs in soybean plants was expected to be quite different.

Both Fe NP-S, Fe-NP-I and commercial Fe NPs were insoluble in deionized water. The solubility of Fe NP-S NPs was 0.29 ± 0.02 %; solubility of Fe NP-I was 0.01 ± 0.001 % and solubility of commercially available Fe NP was 0.06 ± 0.002 %. Thus, NPs produced from *C. sativa* ssp. *sativa* (Fe NP-S) released 20-fold more ions in water than NPs synthesized using ssp. *indica* extract (Fe NP-I) (Figure S2). Given that far more alkanes and alkenes were associated with NPs synthesized from ssp. *indica* (Figures 2 and 3), the resulting difference in polarity might explain the lower nanoparticle dissolution.

The Fe content of commercially available Fe NP was 48.54 ± 0.96 %, while that in the biosynthesized Fe NPs was 37.03 ± 2.19 % in Fe NP-S and 36.63 ± 4.20 % in Fe NP-I. This implies that plants received approximately 98 mg/L of Fe when commercial Fe NPs were applied; while 81 mg/L and 82 mg/L were supplied with Fe NP-S and Fe NP-I, respectively. This is about 17-18% more Fe in the commercial Fe NPs than the biogenic NPs. Given this, it could be assumed that the NPs differential effects on the soybean plants (discussed below) depended mainly on differences in their characteristics, which allowed the biogenic NPs to produce specific advantages over their commercial counterpart even at almost 20% lower nominal Fe dose.

Effect of hemp-synthesized Fe NPs on soybean biomass

Fe NP-S treatment increased soybean shoot and root biomasses by 148 and 264 %, respectively, compared to the control (Figure 5A). Notably, these increases were significantly greater than obtained with the commercial NPs, which were 109 % increase in shoot mass, and 127 % increase in root mass compared to control plants. Cao *et al*.[36] and Dola *et al*.[37] also reported an increase in soybean growth following foliar addition of Fe NPs using a wide concentration range (10 - 200 mg/L). However, no impact on biomass was observed with the Fe NP-I treatment (Figure 5B). In addition, the biomass of plants treated with iron acetate was 156% and 122% lower for shoot and root mass, respectively, compared to control plants (Figure 5B). Taken together, these results suggest that differences in plant compounds capping the surface of the green-synthesized Fe NPs could be contributing to the plant growth stimulating effect of these particles. The difference in the effects of ionic Fein the two experiments, might be due to initial better health of plants in the experiment with Fe NP-I compared to the plants in the experiment with Fe NP-S (mainly due to the change in light quality), which means less Fe was needed for normal functioning, such that extra Fe caused slight phytotoxicity. These results are supported by the findings of Faizan et al.[22] and Harish et al[29] who reported that in optimal conditions, the addition of Fe in ionic form could have detrimental effects on the plant.

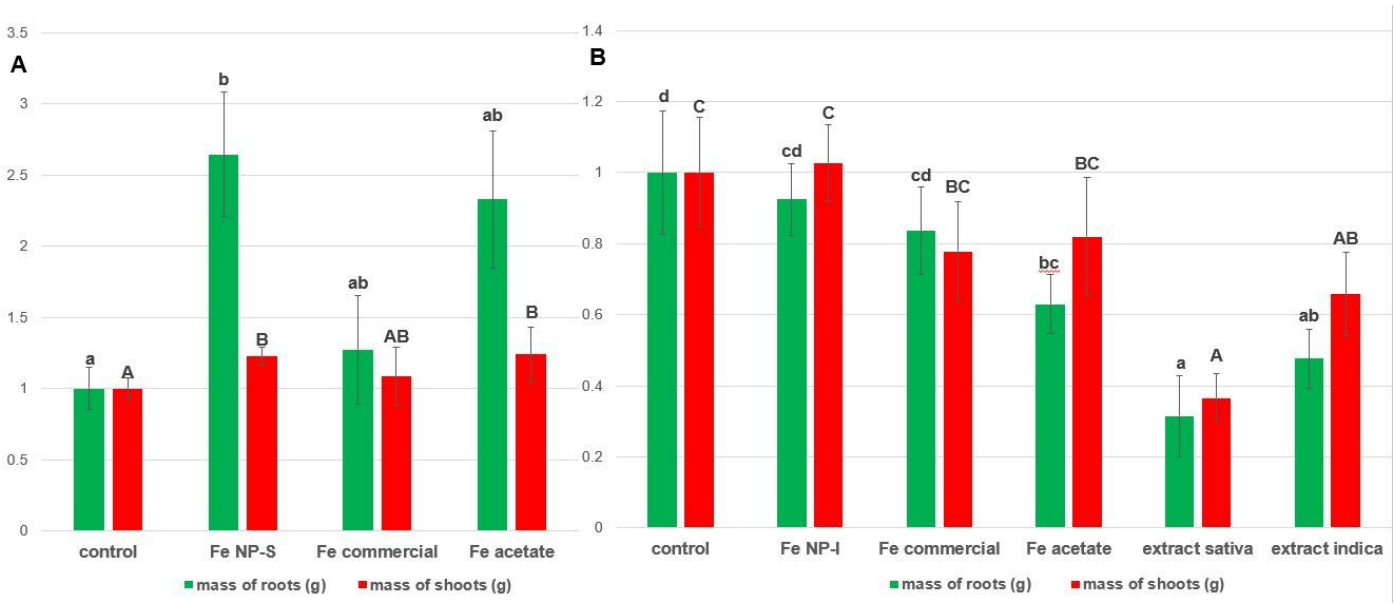

Figure 5. Changes in normalized biomass of soybean exposed to Fe NPs. A- Experiment with iron nanoparticles synthesized from *Cannabis sativa* ssp. *sativa* extract; B- Experiment with iron nanoparticle synthesized from *Cannabis sativa* ssp. *indica* extract. Fe NP-S - Fe nanoparticles synthesized from Cannabis sativa ssp. sativa extract; Fe commercial- commercial Fe_2O_3 nanoparticles; Fe NP-I - Fe nanoparticles synthesized from *Cannabis sativa* ssp. *indica* extract; extract sativa- *Cannabis sativa* ssp. *sativa* extract; extract indica- *Cannabis sativa* ssp. *indica* extract. Different letters indicate that samples were statistically different (as determined by Tukey test at $p < 0.05$).

Effect of hemp-synthesized Fe NPs on total plant chlorophyll content

Figure 6 shows changes in total chlorophyll content upon application of Fe NPs synthesized from *Cannabis sativa*, as well as the commercial Fe NPs. Three weeks after treatment, the total chlorophyll content in soybean plants treated with Fe NP-S, Fe NP-I and commercial Fe NPs increased by 123 %, 114 % and 109 %, respectively, compared to the unamended controls. The increase in total chlorophylls content with Fe NP-S and Fe NP-I was statistically significant, whilst addition of commercial Fe NPs was not statistically significant. The application of iron acetate used as ionic control had no impact on chlorophyll content in either experiment. The largest increase in chlorophyll content in each experiment was observed during the first week and might be due to initial adaptation of the plants to the treatments. Subsequently, the plants attained homeostasis and differences in the pigment content were of a lesser magnitude. A similar trend was observed for several other physiological parameters (Figures 7-9; Figures S3-S6). Extracts from ssp. *sativa* and ssp. *indica* had lower chlorophylls content compared to controls, but these results might be explained by the presence of ethanol in the extract that dehydrated the leaf surface. These results agree with those reported by Dola et al.[37] and Ghafariyan et al.[43] for nanoscale Fe_2O_3 and Fe_3O_4 in soybean.

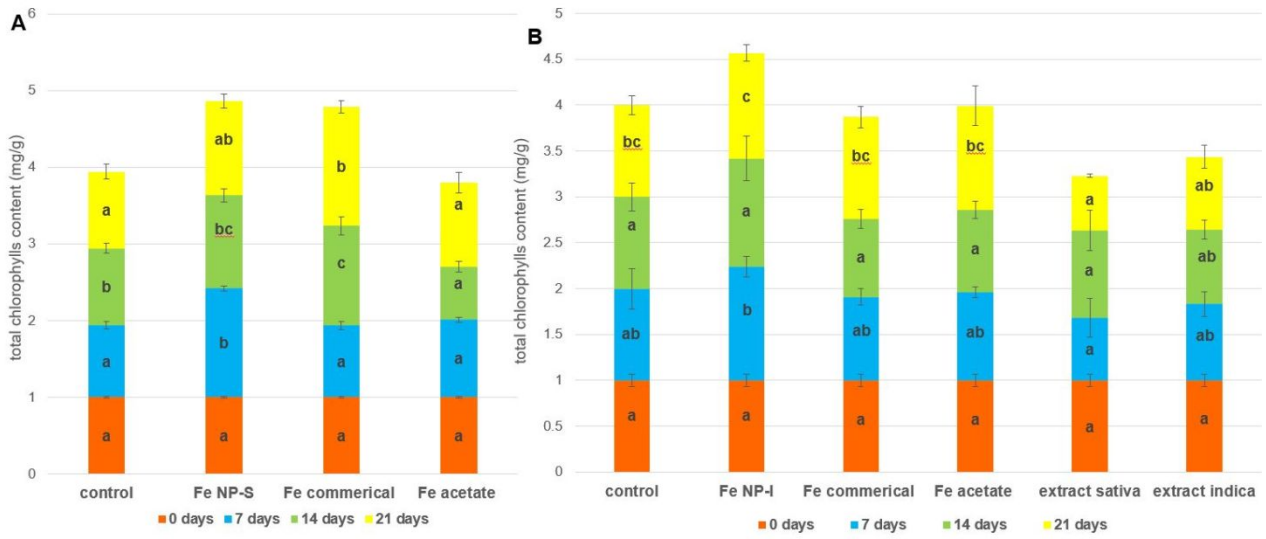

Figure 6. Changes in normalized total chlorophylls content in soybean exposed to Fe NPs. A- Experiment with iron nanoparticles synthesized from Cannabis sativa ssp. sativa extract; B- Experiment with iron nanoparticle synthesized from *Cannabis sativa* ssp. *indica* extract. Fe NP-S - Fe nanoparticles synthesized from *Cannabis sativa* ssp. *sativa* extract; Fe commercial- commercial Fe_2O_3 nanoparticles; Fe NP-I - Fe nanoparticles synthesized from *Cannabis sativa* ssp. *indica* extract; extract sativa- *Cannabis sativa* ssp. *sativa* extract; extract indica- *Cannabis sativa* ssp. indica extract. Different letters indicate that samples were statistically different (as determined by Tukey test at $p < 0.05$).

Effect of hemp-synthesized Fe NPs on plant antioxidant content

Antioxidants play a crucial role in protecting plants against the harmful effects of radical oxygen (or nitrogen) species, usually by transferring electron(s) and hydrogen atoms to free radicals, thereby stabilizing them in the process. Different assays testing for antioxidant content exhibit different sensitivities towards different classes of antioxidants, based on their polarity. Therefore, 2,2-diphenyl-1-picrylhydrazyl (DPPH) and 2,2'-azino-bis(3-ethylbenzothiazoline-6-sulfonic acid) (ABTS) assays were done to assess the content of nonpolar and polar antioxidant compounds, respectively (Figure 7 and Figure S3). Both Fe NPs synthesized from the different subspecies of hemp showed significant potential to increase antioxidant content in soybean (Figure 8 A and B) compared to the respective control plants and commercial Fe NPs. Three weeks following exposure, plants treated with Fe NP-S showed significantly higher antioxidant content compared to the control plants (increase of 151 %) (Figure 7A). Treatment with Fe NP-I was less efficient than treatment with Fe NP-S, increasing antioxidant content by 119 %, which was also statistically significant (Figure 7B). Observed differences between the hemp-derived NPs were likely due to several factors, including greater effect of compounds in the extract from ssp. sativa compared to extract from ssp. *indica* and their greater dissolution (Figure S2).

Plants treated with commercial Fe NPs were more efficient than Fe NP-I at increasing antioxidant content (129 % increase, which was statistically significant), but less effective than Fe NP-S (120% increase in antioxidant content compared to control plants). Plants treated with iron acetate in both cases had antioxidant content similar to those of the control plants (Figure 7 A and B). Feng et al.[29] also found that exposure to Fe_3O_4 NPs at 200 mg/l via foliar application increased the antioxidant content in wheat.

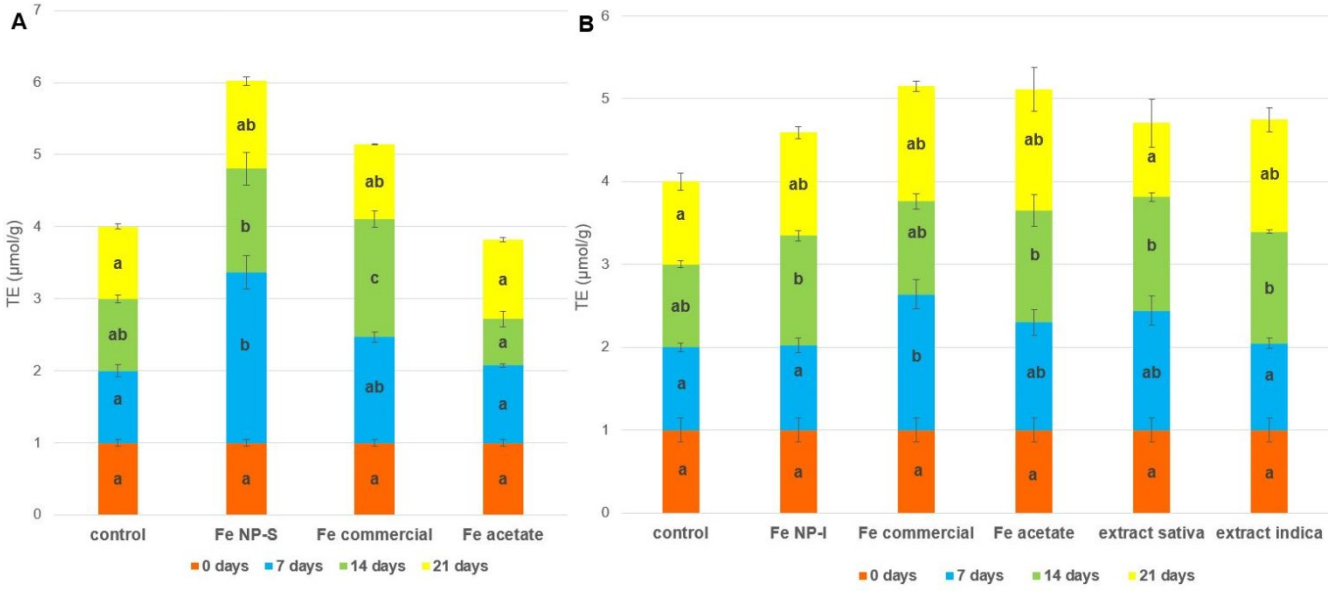

Figure 7. Changes in normalized antioxidant content in soybean exposed to Fe NPs (as detected by DPPH assay). A- Experiment with iron nanoparticles synthesized from *Cannabis sativa* ssp. *sativa* extract; B- Experiment with iron nanoparticle synthesized from *Cannabis sativa* ssp. *indica* extract. Fe NP-S - Fe nanoparticles synthesized from *Cannabis sativa* ssp. *sativa* extract; Fe commercial- commercial Fe_2O_3 nanoparticles; Fe NP-I - Fe nanoparticles synthesized from *Cannabis sativa* ssp. *indica* extract; extract sativa- *Cannabis sativa* ssp. *sativa* extract; extract indica - *Cannabis sativa* ssp. *indica* extract. Different letters indicate that samples were statistically different (as determined by Tukey test at $p < 0.05$).

Results obtained with the ABTS assay (Figure S3) were similar to those obtained by DPPH assay. The extract from ssp. *sativa* had more impact on antioxidant content than that from ssp. *indica* (Figure S3 B) and plants treated with both extracts had statistically higher antioxidant content compared to the untreated control (184 % increase for ssp. *sativa* and 125 % increase for ssp. *indica*). These results suggest that plant compounds from the extracts themselves play a role in stimulating antioxidant synthesis in soybean and contribute to the effects observed with the hemp-derived NPs.

Effect of hemp-synthesized Fe NPs on plant cell viability

Plant cell viability assay measures the activity of electron-transport chain and, therefore, the ability of the cell to produce energy. Since Fe is a cofactor of several oxidoreductases involved in electron transport in the respiratory chain,[24-27] addition of Fe is expected to positively impact plant cell viability. In plants treated with biosynthesized Fe NPs, cell viability increased by 111 % in treatment with Fe NP-S and by 116 % in treatment with Fe NP-I when compared to their respective control plants (Figure S4 A and B). On the other hand, the addition of commercial NPs and the ion treatment had no statistically significant impact on plant cell viability (Figure S4). These findings suggest that the impact of biosynthesized Fe NPs could be attributed to the presence of NP-associated biomolecules that stimulate cellular respiration.

Effect of hemp-synthesized Fe NPs on total polyphenolic content

Polyphenols play protective roles in plants by providing defense against ultraviolet radiation, certain pathogens, and free radicals. In both experiments (Figures S5A and S5B), ionic Fe had a stronger impact on the content of polyphenols than the biosynthesized NPs. From the treatments with biosynthesized NPs, only Fe NP-S addition increased total polyphenolic content (TPC) significantly (116 % increase compared to control plants), while Fe NP-I treatment didn't have statically significant impact (105 % increase compared to the control plants). Treatment with commercial NPs significantly increased TPC in the experiment with Fe NP-S, but not in the experiment with Fe NP-I. A possible explanation for such differences is the statistically significant difference in the initial total polyphenolic content in the plants (7672.3 ± 750.4 GAE (μg/g) in the experiment with Fe NP-S and 8039.4 ± 162.5 GAE (μg/g) in the experiment with Fe NP-I). These results might suggest that there is a polyphenolic content threshold in the plant, which, once reached further addition of iron may have no effect unless the plant experiences additional stress. Berrios et al.[51] also found that foliar addition of 100 mg/L of iron nanoparticle encapsulated in alginate beads increased polyphenolic content in the lettuce. Also, the observed differences in efficacy of ionic Fe treatment and treatment with NPs may be due to absorption of polyphenols on the surface of Fe_3O_4 NPs[55] (e.g. formation of iron-polyphenols complexes) which would decrease the content of free, soluble polyphenols which is determined by the Folin – Ciocalteu assay.

Effect of hemp-synthesized Fe NPs on malondialdehyde content

Malondialdehyde (MDA) is an intermediate compound produced as the result of membrane lipid peroxidation. As such MDA is a strong indicator of oxidative stress.[56] As evident from Figure S6, the largest change in MDA content in both experiments occurred during the first week, which was due to sudden influx of Fe and plants' adaption to the treatment. Notably, Fe NP-S application significantly increased the MDA content by 158 % compared to the control plants. This membrane stress may be due to the particles' positive charge that disrupted the membrane potential, as well as the larger hydrodynamic diameter and higher dissolution rate (Table S3 and Figure S2). Barbasz et al.[57] also found that foliar application of positively charged silver NPs (zeta potential -approximately +50 mV at pH 7) even at a low dose of 10 mg/L increased the lipid peroxidation in wheat seedlings by

100% compared to nontreated seedlings. This increase in lipid peroxidation was more than 10% higher than the increase detected in the treatment with negatively charged silver NPs (zeta potential – 30 mV at pH 7). For the more stable and negatively charged Fe NP-I, MDA content significantly decreased (134% compared to the control), which agrees with previously discussed data.[57] Feng et al.[29] found that treatment with Fe3O4 NPs decreased MDA content in wheat. In both experiments, the ionic Fe treatment caused greater lipid peroxidation than the nanoparticle treatments. It is probable that dissolution rate was a major factor in membrane damage.

Effect of hemp-synthesized Fe NPs reduced glutathione content

Glutathione counteracts oxidative stress caused by either biotic or abiotic factors by preventing the formation of free radicals. In this process, glutathione is transformed from its reduced form (GSH) to an oxidized form (GSSG). Thus, a higher presence of GSH indicates high reductive potential and, therefore, greater plant tolerance to stress.[58]The addition of Fe NP-S and Fe NP-I significantly increased GSH content in soybean plants by 137 % and 110 % compared to the control plants, respectively (Figure S7). Both biosynthesized Fe NPs were more efficient in elevating GSH content when compared to the commercial Fe NPs and the corresponding Fe ions (Figure S6 A and B). In fact, in the experiment with Fe NP-I, addition of commercial Fe NPs decreased GSH content, which might suggest that commercially available NPs were transported faster than biosynthesized ones, leading to the high Fe content. These results agree with Fazal *et al.*[24] and Cao *et al*.[37], who reported that treatment of healthy plants grown under optimal conditions with Fe could be detrimental to growth and ability to withstand oxidative stress. Additionally, some of the effects ascribed to the green-synthesized NPs could have been from the hemp metabolites capping the nanoparticle surface, given that the extracts themselves seemed to impact GSH content, although non-significantly (Figure S6 B). Some of the compounds that might influence GSH content due to their synergistic activities in plants are terpenes[55] and phenols,[56] which are notably present in the extracts.

Effect of hemp-synthesized Fe NPs on the activities of antioxidative enzymes

Figures S8, S9 and 8 represent the activities of catalase (CAT), peroxidase (POX), and superoxide dismutase (SOD), respectively. Given that the role of these enzymes is to capture free radicals prior to damage of cellular components, their increased activity is generally considered to be reflective of a higher level of oxidative stress in the plant. Similar to the results obtained for antioxidant content, all enzymes showed significant increases in activity in the first week of treatment, which is probably due to the activation of defense mechanisms in response to treatment. However, 3 weeks after the treatment with biosynthesized NPs, the activities of these enzymes decreased compared to the control plants, and the decreases in CAT and SOD were more significant than that of POX. Specifically, Fe NP-S significantly decreased CAT activity by 133 %, whereas Fe NP-I significantly decreased both CAT and SOD activity by 142 and 136%, respectively. Feng *et al*.[29] and El-Amine *et al*.[27] also reported decreases

in SOD activity in wheat and soybean treated with Fe NPs (foliar application, dose - 200 mg/L). However, the application of commercial Fe NPs had the opposite effect on SOD activity. In the experiment with Fe NP-S, SOD activity significantly increased by 131 %, while in the experiment with Fe NP-I activities increased by 111 %, compared to controls. These findings align with the results of Faizal *et al.*[24] showing that a high concentration (500 mg/l) of Fe NPs can increase oxidative stress in the plant. A possible reason why this stress response is not triggered with green NPs could be the protective effect of the plant compounds capping the surface of the NPs. Similar to GSH content, compounds associated with a decrease in SOD activity and that were present on the surface of biosynthesized NPs include terpenes[58] and phenols.[59]

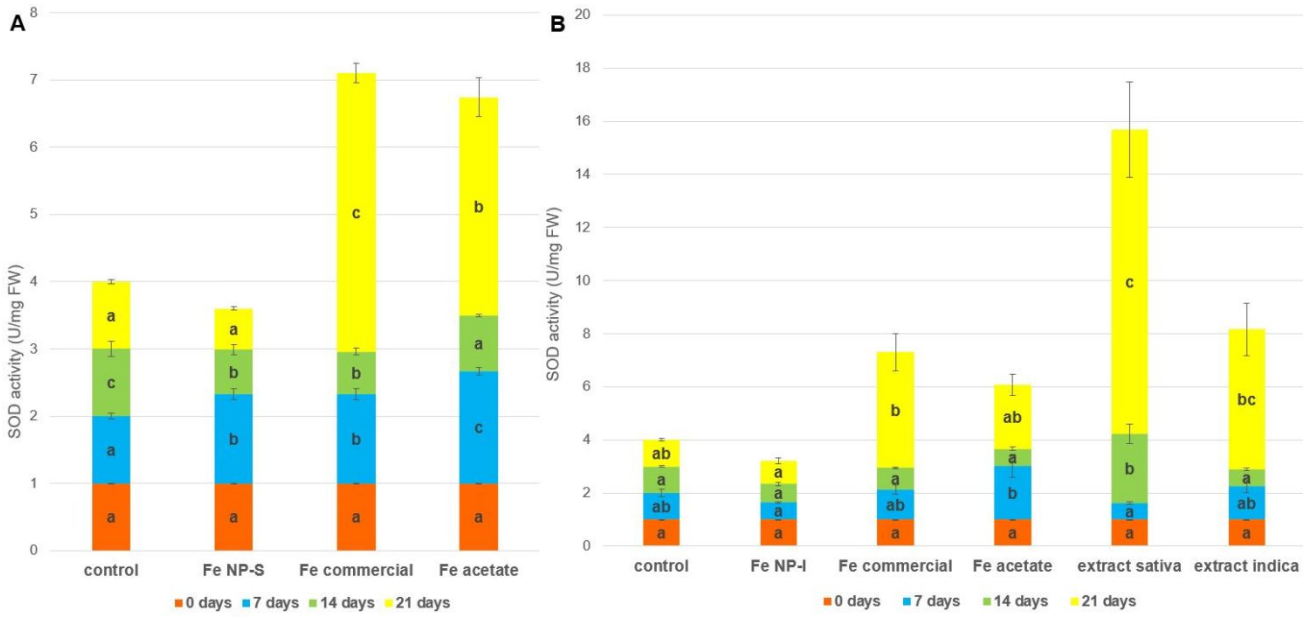

Figure 8. Changes in normalized superoxide dismutase activity in soybean exposed to Fe NPs. A- Experiment with iron nanoparticles synthesized from *Cannabis sativa* ssp. *sativa* extract; B- Experiment with iron nanoparticle synthesized from *Cannabis sativa* ssp. *indica* extract. Fe NP-S - Fe nanoparticles synthesized from *Cannabis sativa* ssp. *sativa* extract; Fe commercial- commercial Fe_2O_3 nanoparticles; Fe NP-I - Fe nanoparticles synthesized from *Cannabis sativa* ssp. *indica* extract; extract sativa- *Cannabis sativa* ssp. *sativa* extract; extract indica- *Cannabis sativa* ssp. *indica* extract. Different letters indicate that samples were statistically different (as determined by Tukey test at $p < 0.05$).

Shoot to root translocation of Fe from hemp-synthesized Fe NPs

The translocation of iron depended on several factors including size, shape and surface charge of the original NPs and type of the plant.[61] Smaller NPs (less than 30 nm) are transported faster from shoots to roots and vice versa, due to the possibility to be

absorbed and transferred by the stomata.[62,63] Additionally, when applied foliarly, positively-charged NPs are absorbed faster than negatively-charged ones, due to the electrostatic attraction between positively-charged NPs and negatively-charged cell wall.[60] Given that Fe NP-S were positively charged and Fe NP-I were smaller (Table S3), it seems that those factors were counteractive, such that translocation factors were relatively similar (173% and 170% higher than control plants) (Figure S10). However, the translocation factor for the commercial Fe NPs was significantly higher than for biosynthesized NPs in both experiments. These results might indicate that the presence of plant-derived compounds on the surface of NPs inhibits transport of the NPs from shoots to roots. These findings were confirmed by the fact that translocation factors for the sativa and indica extract were higher than for control plants, although not significantly. The highest translocation factor in both experiments was observed for ionic Fe, which is due to the rapid dissociation of the salt form in water and fast binding of Fe^{2+} ions to iron transporters. A previous study showed that plant compounds like organic acids could facilitate NP solubilization at high doses, and that the plant compound-coated NPs could be affected in their ability to elicit biological responses compared to ions [64], due likely to reduced exposure to dissolved ions from the NPs, or reduced transportation of intact NPs.

CONCLUSIONS

Soybean plants treated with iron NPs synthesized from hemp waste exhibited increased biomass, viability, content of chlorophylls, antioxidants and reduced glutathione compared to untreated controls and plants treated with commercial iron NPs. However, these effects varied based on subspecies of hemp used for nanoparticle synthesis. Clear differences in NP charge, hydrodynamic size, and dissolution rate were evident as a function of *Cannabis sativa* subspecies, and these differences impacted the extent and nature of plant response. Specifically, given that Fe NP-S had higher impact that Fe NP-I on the content of chlorophylls, antioxidants and polyphenols, it is possible that residual alcohols (including phenols and sterols) and mercaptans contributed to the increase in the rate of photosynthesis rate and increased content of different classes of antioxidants. Conversely, Fe NP-I had more impact than Fe NP-S on the increase in viability and decrease in MDA content and activity of antioxidant enzymes. These results might imply that residual amines, organic acids and esters played a role in enhancing activity in respiratory chain and plant's response to reactive oxygen species. This study demonstrates the potential of synthesizing plant-efficient iron-based nanofertilizers from hemp waste, thereby corroborating existing reports on the unique properties and efficacy of plant-derived metal oxide NPs. However, the subspecies differences in their secondary metabolite profile clearly confer significant control over the resulting NPs properties, including charge, size, dissolution profile and impact on the treated plant. Hence, a thorough understanding of these differences in candidate plants is critical for plant waste material preference, selection, and successful upscaling of NP synthesis using such plant materials. Further time-dependent molecular-level studies are needed to understand how plant material residues affect the bioactivity of hemp-derived iron NPs, including assessing the safety of this

approach. Overall, these findings demonstrate the unique potential of plant-waste derived micronutrient NPs as an important nano-enabled strategy to enhance agricultural productivity. Additionally, due to the low cost of synthesis of "green" Fe_3O_4 NPs from plant waste, this procedure is more economical compared to application of commercial Fe-based fertilizers. Additional analyses are necessary to assess the effects of biosynthesized Fe NPs on soil microbiota and nanoparticles persistence in the soil.

CONFICT OF INTEREST

There are no conflicts to declare.

DATA AVAILABILITY STATEMENT

Data for this article are available at Open Science Framework at https://osf.io/sncmq/

ACKNOWLEDGMENT

This work is supported by USDA NIFA AFRI 2023-67021-39747. The authors would like to thank Meghan Cahill, Jingyi Zhou and Michael Ammirata for the help with experiment analysis. We are also grateful to the Connecticut Consumer Protection – Drug Control Division and Advanced Grow Labs for kindly providing us with *Cannabis sativa* (ssp. *indica*) leaves and stem.

Supplementary material

Table S1: Wavenumber range assigned to different bonds and compounds; Table S2: Composition of extract from *Cannabis sativa* ssp. *sativa* and *Cannabis sativa* ssp. *indica*; Table S3: Zeta potential, hydrodynamic diameter and dry size of nanoparticles synthesized using *Cannabis sativa* ssp. *sativa* (Fe NP-S) and Cannabis sativa ssp. indica (Fe NP-I); Figure S1. Transmission electron micrographs of iron nanoparticles. A-Iron nanoparticles synthesized from *Cannabis sativa* ssp. *sativa*; B- Iron nanoparticles synthesized from *Cannabis sativa* ssp. *indica*; Figure S2**.** Dissolution analysis of iron nanoparticles. Fe NP-S - Iron nanoparticles synthesized from *Cannabis sativa* ssp. *sativa*; Fe NP-I- Iron nanoparticles synthesized from *Cannabis sativa* ssp. *Indica;* Fe commercial NP - commercially available iron oxide nanoparticles; Figure S3. Changes in normalized antioxidant content in soybean exposed to Fe NPs (as detected by ABTS assay). A- Experiment with iron nanoparticles synthesized from *Cannabis sativa* ssp. *sativa* extract; B- Experiment with iron nanoparticle synthesized from *Cannabis sativa* ssp. *indica* extract. Fe NP-S - Fe nanoparticles synthesized from *Cannabis sativa* ssp. *sativa* extract; Fe commercial- commercial Fe_2O_3 nanoparticles; Fe NP-I - Fe nanoparticles synthesized from *Cannabis sativa* ssp. *indica* extract; extract sativa- *Cannabis sativa* ssp. *sativa* extract; extract indica- *Cannabis sativa* ssp. *indica* extract. Different letters indicate that samples were statistically different (as determined by Tukey test at $p < 0.05$); Figure S4. Changes in normalized plant cell viability in soybean exposed to Fe NPs. A- Experiment with iron nanoparticles synthesized from *Cannabis sativa* ssp. *sativa* extract; B- Experiment with iron nanoparticle synthesized from

Cannabis sativa ssp. *indica* extract. Fe NP-S - Fe nanoparticles synthesized from *Cannabis sativa* ssp. *sativa* extract; Fe commercial- commercial Fe2O3 nanoparticles; extract sativa- *Cannabis sativa* ssp. *sativa* extract; Fe NP-I - Fe nanoparticles synthesized from *Cannabis sativa* ssp. *indica* extract; extract indica- *Cannabis sativa* ssp. *indica* extract. Different letters indicate that samples were statistically different (as determined by Tukey test at $p < 0.05$); Figure S5**.** Changes in normalized total polyphenolic content in soybean exposed to Fe NPs. A- Experiment with iron nanoparticles synthesized from *Cannabis sativa* ssp. *sativa* extract; B- Experiment with iron nanoparticle synthesized from *Cannabis sativa* ssp. *indica* extract. Fe NP-S - Fe nanoparticles synthesized from *Cannabis sativa* ssp. *sativa* extract; Fe commercial- commercial Fe_2O_3 nanoparticles; Fe NP-I - Fe nanoparticles synthesized from *Cannabis sativa* ssp. *indica* extract; extract sativa- *Cannabis sativa* ssp. *sativa* extract; extract indica- *Cannabis sativa* ssp. *indica* extract. Different letters indicate that samples were statistically different (as determined by Tukey test at $p < 0.05$).

Figure S6. Changes in normalized malondialdehyde content in soybean exposed to Fe NPs. A- Experiment with iron nanoparticles synthesized from *Cannabis sativa* ssp. *sativa* extract; B- Experiment with iron nanoparticle synthesized from *Cannabis sativa* ssp. *indica* extract. Fe NP-S - Fe nanoparticles synthesized from *Cannabis sativa* ssp. *sativa* extract; Fe commercial- commercial Fe_2O_3 nanoparticles; Fe NP-I - Fe nanoparticles synthesized from *Cannabis sativa* ssp. *indica* extract; extract sativa- *Cannabis sativa* ssp. *sativa* extract; extract indica- *Cannabis sativa* ssp. *indica* extract. Different letters indicate that samples were statistically different (as determined by Tukey test at $p < 0.05$); Figure S7. Changes in normalized glutathione content in soybean exposed to Fe NPs. A- Experiment with iron nanoparticles synthesized from *Cannabis sativa* ssp. *sativa* extract; B- Experiment with iron nanoparticle synthesized from *Cannabis sativa* ssp. *indica* extract. Fe NP-S - Fe nanoparticles synthesized from *Cannabis sativa* ssp. *sativa* extract; Fe commercial- commercial Fe_2O_3 nanoparticles; Fe NP-I - Fe nanoparticles synthesized from *Cannabis sativa* ssp. *indica* extract; extract sativa- *Cannabis sativa* ssp. *sativa* extract; extract indica- *Cannabis sativa* ssp. *indica* extract. Different letters indicate that samples were statistically different (as determined by Tukey test at $p < 0.05$); Figure S8. Changes in normalized catalase activity in soybean exposed to Fe NPs. A- Experiment with iron nanoparticles synthesized from *Cannabis sativa* ssp. *sativa* extract; B- Experiment with iron nanoparticle synthesized from *Cannabis sativa* ssp. *indica* extract. Fe NP-S - Fe nanoparticles synthesized from *Cannabis sativa* ssp. *sativa* extract; Fe commercial- commercial Fe_2O_3 nanoparticles; Fe NP-I - Fe nanoparticles synthesized from *Cannabis sativa* ssp. *indica* extract; extract sativa- *Cannabis sativa* ssp. *sativa* extract; extract indica- *Cannabis sativa* ssp. *indica* extract. Different letters indicate that samples were statistically different (as determined by Tukey test at $p < 0.05$); Figure S9. Changes in normalized peroxidase activity in soybean exposed to Fe NPs. A- Experiment with iron nanoparticles synthesized from *Cannabis sativa* ssp. *sativa* extract; B- Experiment with iron nanoparticle synthesized from *Cannabis sativa* ssp. *indica* extract. Fe NP-S - Fe nanoparticles synthesized from *Cannabis sativa* ssp. *sativa* extract; Fe commercial- commercial Fe_2O_3 nanoparticles; Fe NP-I - Fe nanoparticles synthesized from *Cannabis sativa* ssp. *indica* extract; extract sativa- *Cannabis sativa* ssp.

sativa extract; extract indica- *Cannabis sativa* ssp. *indica* extract. Different letters indicate that samples were statistically different (as determined by Tukey test at $p < 0.05$); Figure S10. Translocation factor of Fe NPs in soybean. A- Experiment with iron nanoparticles synthesized from *Cannabis sativa* ssp. *sativa* extract; B- Experiment with iron nanoparticle synthesized from *Cannabis sativa* ssp. *indica* extract. Fe NP-S - Fe nanoparticles synthesized from *Cannabis sativa* ssp. *sativa* extract; Fe commercial- commercial Fe_2O_3 nanoparticles; Fe NP-I - Fe nanoparticles synthesized from *Cannabis sativa* ssp. *indica* extract; extract sativa- *Cannabis sativa* ssp. *sativa* extract; extract indica- *Cannabis sativa* ssp. *indica* extract. Different letters indicate that samples were statistically different (as determined by Tukey test at $p < 0.05$).

References

1. H. Singh, M.F. Desimone, S. Pandya, S. Jasani, N. George, M. Adnan, A. Aldarhami, A.S. Bazaid and S.A. Alderhami. Revisiting the Green Synthesis of Nanoparticles: Uncovering Influences of Plant Extracts as Reducing Agents for Enhanced Synthesis Efficiency and Its Biomedical Applications. *Int. J. Nanomedicine*. 2023, **18**, 4727-4750.

2. S. Ying, Z. Guan, P.C. Ofoegbu, P. Clubb, C. Rico, F. He and Hong, J. Green Synthesis of Nanoparticles: Current Developments and Limitations. *Environ. Technol.* 2022, **26**, 102336.

3. A. Khosravi, A. Zarepour, S. Iravani, R. S. Varma and A. Zarrabi. Sustainable synthesis: natural processes shaping the nanocircular economy. *Environ. Sci.: Nano*, 2024,**11**, 688-707.

4. M.S. Haydar, P. Saha, P. Mandal and S. Roy. Evaluating the impact of phytosynthesized micronutrient nanoparticles on the growth and propagation of mulberry cuttings: dose determination and toxicity concerns. *Environ. Sci.: Nano*, 2024,**11**, 1179-1203.

5. M.S. Aida, N. Alonizan, B. Zarrad and M. Hjiri. Green Synthesis of Iron oxide Nanoparticles using Hibiscus Plant Extract. *J. Taibah Univ. Sci.* 2023, **17(1**), 2221827.

6. H.F. Kiwumulo, H. Muwonge, C. Ibingira, C. Lubwama, J.B. Kirabira and R.T. Ssekitoleko. Green Synthesis and Characterization of Iron-oxide Nanoparticles using Moringa Oleifera: a Potential Protocol for Use in Low and Middle Income Countries. *BMC Res Notes* 2022, **15**, 149.

7. S. Khan, G. Bibi, S. Dilbar, A. Iqbal, M. Ahmad, A. Ali, Z. Ullah, M. Jaremko, J. Iqbal, M. Ali, I. Haq, and I. Ali. Biosynthesis and Characterization of Iron Oxide Nanoparticles from Mentha Spicata and Screening Its Combating Potential Against Phytophthora Infestans. *Front. Plant Sci.* 2022, **13**,1001499.

8. F. Buarki, H. AbuHassan, F. Al Hannan and F. Z. Henari. Green Synthesis of Iron Oxide Nanoparticles Using Hibiscus Rosa Sinensis Flowers and Their Antibacterial Activity. *J. Nanotechnol.* 2022, 5474645.

9. M.H. Nahari, A. Al Ali, A. Asiri, M.H. Mahnashi, I.A. Shaikh, A.K. Shettar and J. Hoskeri. Green Synthesis and Characterization of Iron Nanoparticles Synthesized from Aqueous Leaf Extract of Vitex Leucoxylon and Its Biomedical Applications. *Nanomaterials* 2022, **12**, 2404.

10. S. Saif, A. Tahir and Y. Chen. Green Synthesis of Iron Nanoparticles and Their Environmental Applications and Implications. *Nanomaterials* 2016, **6(11),** 209.

11. L.H. Tan, C.Y. Lim, L.Y. Ng and Y.P lim. Plant-Mediated Synthesis of Iron Nanoparticles for Environmental Application: Mini Review. *Mater. Today Proc.* 2023, **87(**2), 64-69.

12. G. López-Téllez, P. Balderas-Hernández, C.E. Barrera-Díaz, A.R. Vilchis-Nestor, G. Roa-Morales and B. Bilyeu. Green Method to Form Iron Oxide Nanorods in Orange Peels for Chromium (VI) Reduction. *J Nanosci Nanotechnol.* 2013, **13(3),** 2354-2361.

13. S. Venkateswarlu, Y. S. Rao, T. Balaji, B. Prathima and N.V.V. Jyothi. Biogenic Synthesis of Fe_3O_4 Magnetic Nanoparticles using Plantain Peel Extract. *Mater. Lett.* 2013, **100**, 241–244.

14. J.A.A. Abdullah, S.N.P. Lagos, E.J.E. Sanchez, O. Rivera-Flores, M. Sánchez-Barahona, A. Guerrero and A. Romero. Innovative Agrowaste Banana Peel Extract-based Magnetic Iron Oxide Nanoparticles for Eco-friendly Oxidative Shield and Freshness Fortification. *Food Bioprocess Technol*. **2024**.

15. S. Huang, H. Li, J. Xu, H. Zhou, N.P. Seeram, H. Ma and Q Gu. Chemical Constituents of Industrial Hemp Roots and Their Anti-Inflammatory Activities. *J. Cannabis Res.* 2023, **5(1),** 1.

16. A.J. Josiah, S.K. Pillai, W. Cordier, M. Nell, D. Twilley, N. Lall and S.S. Ray. Cannabidiol-Mediated Green Synthesis, Characterization, and Cytotoxicity of Metal Nanoparticles in Human Keratinocyte Cells. *ACS Omega*. **2021**, 6(43), 29078-29090.

17. A. Judžentienė, R. Garjonytė, and J. Būdienė. Phytochemical Composition and Antioxidant Activity of Various Extracts of Fibre Hemp (Cannabis sativa L.) Cultivated in Lithuania. *Molecules*. 2023, **28(13**), 4928.

18. F. Ahmadi and M. Lackner. Green Synthesis of Silver Nanoparticles from Cannabis sativa: Properties, Synthesis, Mechanistic Aspects, and Applications. *ChemEngineering* 2024, **8**, 64.

19. I. Karmous, S. Vaidya, C. Dimkpa, N. Zuverza-Mena, W. da Silva, K. Alves Barroso, J. Milagres, A. Bharadwaj, W. Abdelraheem, J.C. White and W.H. Elmer. Biologically Synthesized Zinc and Copper Oxide Nanoparticles Using *Cannabis sativa* L. Enhance Soybean (*Glycine max*) Defense Against Fusarium virguliforme. *Pestic. Biochem. Physiol.* 2023, **194**, 105486.

20. N. Korkmaz, D. Kısa, Y. Ceylan, E. Güçlü, F. Şen and A. Karadağ. Synthesis of CeO2 Nanoparticles from Hemp Leaf Extract: Evaluation of Antibacterial, Anticancer and Enzymatic Activities. *Inorg. Chem. Comm.* 2024, **159**, 111797.

21. P. Singh, S. Pandit, J. Garnæs, S. Tunjic, V.R. Mokkapati, A. Sultan, A. Thygesen, A. Mackevica, R.V. Mateiu, A.E. Daugaard, A. Baun and I. Mijakovic. Green Synthesis of Gold and Silver Nanoparticles from Cannabis sativa (Industrial Hemp) and Their Capacity for Biofilm Inhibition. *Int. J. Nanomedicine*. 2018, **13**, 3571-3591.

22. R. Yang, Y. Wang, M. Li and Y. Hong. A New Carbon/Ferrous Sulfide/Iron Composite Prepared By an In Situ Carbonization Reduction Method from Hemp (Cannabis sativa L.) Stems and Its Cr(VI) Removal Ability. *ACS Sustainable Chem. Eng.* 2014, **2(5),** 1270–1279.

23. R. Coşkun, A. Delibaş and D.Y. Karanfil. Metal Ferrite Supported Bio-Nanocomposite from Hemp Biomass and Properties. *Biomass Conv. Bioref.* 2024, **14**, 18523–18537.

24. M. Faizan, Y. Arif, V.D. Rajput, S. Hayat, T. Minkina, S. Maqbool Ahmed, F. Yu, A. Ilgiz and K. Ilgiz. Effects, uptake and translocation of iron (Fe) based nanoparticles in plants. In: *Nanomaterial-Plant Interactions: Toxicity of Nanoparticles in Plants Toxic. Nanoparticles Plants*, eds. Rajput, V. D.; Minkina, T.; Sushkova, S.; Mandzhieva, S. S., Rensing C., Elsevier: Amsterdam, 2022, pp. 193–209.

25. G. R. Rout and S. Sahoo. Role of Iron in Plant Growth and Metabolism. *Rev. agric. sci.* 2015, **3**, 1-24.

26. I.O. Adisa, V.L.R. Pullagurala, J.R. Peralta-Videa, C.O. Dimkpa, W.H. Elmer, J.L. Gardea-Torresdey and J.C. White. Recent advances in nano-enabled fertilizers and pesticides: A critical review of mechanisms of action. *Environ. Sci.: Nano*. 2019,**6**, 2002-2030.

27. B. El Amine, F. Mosseddaq, R. Naciri and A. Oukarroum. Interactive Effect of Fe and Mn Deficiencies on Physiological, Biochemical, Nutritional and Growth Status of Soybean. *Plant Physiol. Biochem.* 2023, **199**, 107718.

28. M.A. Ahmed, S.S. Shafiei-Masouleh, R.M.; Mohsin and Z.K. Salih. Foliar Application of Iron Oxide Nanoparticles Promotes Growth, Mineral Contents, and Medicinal Qualities of Solidago virgaurea L. *J. Soil Sci. Plant Nutr.* 2023, **23**, 2610–2624.

29. Y. Feng, V.D. Kreslavski, A.N. Shmarev, A.A. Ivanov, S.K. Zharmukhamedov, A. Kosobryukhov, M. Yu, S.I. Allakhverdiev and S. Shabala. Effects of Iron Oxide Nanoparticles (Fe3O4) on Growth, Photosynthesis, Antioxidant Activity and Distribution of Mineral Elements in Wheat (Triticum aestivum) Plants. *Plants* 2022, **11**, 1894.

30. Bhardwaj, A.K.; Arya, G.; Kumar, R.; Hamed, L.; Pirasteh-Anosheh, H.; Jasrotia, P.; Kashyap, P.L.; Singh, G.P. Switching to nanonutrients for sustaining agroecosystems and environment: the challenges and benefits in moving up from ionic to particle feeding. *J Nanobiotechnol.* 2022, **20**, 19.

31. A. Kumari and A.K. Chauhan. Iron nanoparticles as a promising compound for food fortification in iron deficiency anemia: a review. *J. Food Sci. Technol.* 2022, **59(9),** 3319-3335.

32. V. Harish, S. Aslam, S. Chouhan, Y. Pratap and S. Lalotra. Iron Toxicity in Plants: A Review. *Int. J. Environ. Clim. Change*. 2023, **13**, 1894-1900.

33. V. Voora, S. Bermudez, H. Le, C. Larrea and E. Luna. Global Market Report. Soybean Prices and Sustainability. **2024**. https://www.iisd.org/system/files/2024-02/2024-global-market-report-soybean.pdf (assessed October 2023)

34. P.T. Hoe, N.C. Mai, L.Q. Lien, N.K. Ban, C.V. Minh, N.H. Chau N.Q. Buu, D.T. Hien, N.T. Van, L.T.T. Hien and T.M. Linh. Germination Responses of Soybean Seeds to Fe, ZnO, Cu and Co Nanoparticle Treatments. *Int. J. Agric. Biol.* 2018, **20**, 1562–1568.

35. M.F. Iannone, M.D. Groppa, M.S. Zawoznik, D.F. Coral, M.B. Fernández van Raap and M.P. Benavides. Magnetite Nanoparticles Coated with Citric Acid Are Not Phytotoxic and Stimulate Soybean and Alfalfa Growth. *Ecotoxicol. Environ. Saf.* 2021, **211**,111942.

36. X. Cao, L. Yue, C. Wang, X. Luo, C. Zhang, X. Zhao, F. Wu, J.C. White, Z. Wang and B. Xing. Foliar Application with Iron Oxide Nanomaterials Stimulate Nitrogen Fixation, Yield, and Nutritional Quality of Soybean. *ACS Nano*. 2022, **16(1),** 1170-1181.

37. D.B. Dola, M.A. Mannan, U. Sarker, M.A.A. Mamun, T. Islam, S. Ercisli, M.H. Saleem, B. Ali, O.L. Pop and R.A. Marc. Nano-iron oxide accelerates growth, yield, and quality of Glycine max seed in water deficits. *Front Plant Sci.* 2022, **13**, 992535.

38. M.S. Cahill, T. Arsenault, T.H. Bui, N. Zuverza-Mena, A. Bharadwaj, K. Prapayotin-Riveros and C.O Dimkpa. Copper stimulation of tetrahydrocannabinol (THC) and cannabidiol (CBD) production in hemp (Cannabis sativa L.) is copper-type, dose, and cultivar-dependent. *J Agric Food Chem.,* 2024, **72**, 6921–6930.

39. T.L. Arsenault, K. Prapayotin-Riveros, M.A. Ammirata, J.C. White and C.O. Dimkpa. Compliance Testing of Hemp (Cannabis sativa L.) Cultivars for Total Delta-9 THC and Total CBD Using Gas Chromatography with Flame Ionization Detection. Plants, 2024, **13**, 519.

40. A. Hussain, M. Yasar, G. Ahmad, M. Ijaz, A. Aziz, M.G. Nawaz, F.A. Khan, H. Iqbal, W. Shakeel, H. Momand, R. Ali, S. Ahmad, H. Shah, M. Nadeem, D. Ahmad, F. Anjum and S. Faisal. Synthesis, characterization, and applications of iron oxide nanoparticles. *Int. J. Health Sci.* 2023,**17(4),**3-10.

41. S. Lakshminarayanan, M.F. Shereen, K.L. Niraimathi, P. Brindha and A. Arumugam. One-pot Green Synthesis of Iron Oxide Nanoparticles from Bauhinia Tomentosa: Characterization and Application Towards Synthesis of 1, 3 Diolein. *Sci Rep*. 2021, **11(1),** 8643.

42. E.S. Madivoli, P.G. Kareru, E.G. Maina, A. O. Nyabola, S. I. Wanakai and J. O. Nyang'au. Biosynthesis of Iron Nanoparticles Using Ageratum conyzoides extracts, Their Antimicrobial and Photocatalytic Activity. *SN Appl. Sci.* 2019, **1**, 500.

43. M.H., Ghafariyan, M.J. Malakouti, M.R. Dadpour, P. Stroeve and M. Mahmoudi. Effects of magnetite nanoparticles on soybean chlorophyll. *Environ Sci Technol.* 2013, **47(18),**10645-10652.

44. Y. Li, C. Liu, J. Zhang, H. Yang, L. Xu, Q. Wang, L. Sack, X. Wu, J. Hou and N. He. Variation in leaf chlorophyll concentration from tropical to cold-temperate forests: Association with gross primary productivity. *Ecol. Indic.* 2018, **85**, 383–389.

45. C. Sánchez-Moreno, J.A. Larrauri and F. Saura-Calixto. A procedure to measure the antiradical efficiency of polyphenols. *J. Sci. Food Agric.* 1998, **76**, 270–276.

46. R. Re, N. Pellegrini, A. Proteggente, A. Pannala, M. Yang and C. Rice-Evans. Antioxidant activity applying an improved ABTS radical cation decolorization assay. *Free Radic. Biol. Med.* 1999, **26**, 1231–1237.

47. M. Shoemaker, I. Cohen and M. Campbell. Reduction of MTT by aqueous herbal extracts in the absence of cells. *J. Ethnopharmacol*. 2004, **93**, 381-384.

48. Á. Cruz-Carrión, L. Calani, M.J.R. de Azua, P. Mena, D. Del Rio, M. Suárez and A. Arola-Arnal. (Poly)phenolic composition of tomatoes from different growing locations and their absorption in rats: a comparative study. *Food Chem.* 2022, **388**,132984.

49. S. Francesca, S. Najai, R. Zhou, G. Decros, C. Cassan, F. Delmas, C.O. Ottosen, A. Barone and M.M. Rigano. Phenotyping to dissect the biostimulant action of a protein hydrolysate in tomato plants under combined abiotic stress. *Plant Physiol Biochem.* 2022, **179**, 32–43.

50. D.F. Shu, L.Y. Wang, M. Duan, Y.S. Deng and Q.W. Meng. Antisense mediated depletion of tomato chloroplast glutathione reductase enhances susceptibility to chilling stress. *Plant Physiol Biochem*. 2011, **49(10)**, 1228–1237.

51. L. Paesano, A. Perotti, A. Buschini, C. Carubbi, M. Marmiroli, E. Maestri, S. Iannotta and N. Marmiroli. Markers for toxicity to HepG2 exposed to cadmium sulphide quantum dots; damage to mitochondria. *Toxicology*. 2016, **374**, 18–28.

52. O. Çelik, A. Ayan and Ç. Atak. Enzymatic and non-enzymatic comparison of two different industrial tomato (*Solanum lycopersicum*) varieties against drought stress. *Bot Stud.* 2017, **58(1)**, 32.

53. B. Parra-Torrejón, M. Salvachúa-de la Fuente, M.J. Giménez-Bañón, J.D. Moreno-Olivares, J.A. Bleda-Sánchez, D.F. Paladines- Quezada, R. Gil-Muñoz, G.B. Ramírez-Rodríguez and J.M. Delgado-López. Amorphous vs. nanocrystalline calcium phosphate as efficient nanocarriers of elicitors in vineyards. *CrystEngComm*, 2023, **25**, 2372-2378.

54. D. Berríos, J. Nahuelcura, F. González, F. Peña, P. Cornejo, J. Pérez-Navarro, S. Gómez-Alonso and A. Ruiz. The biosynthesis, accumulation of phenolic compounds and antioxidant response in *Lactuca sativa* L. plants inoculated with a biofertilizer based on soil yeast and iron nanoparticles. *Plants* 2024, **13**, 388.

55. A.E. Matías-Reyes, M.L. Alvarado-Noguez, M. Pérez-González, M.D. Carbajal-Tinoco, E. Estrada-Muñiz, J.A. Fuentes-García, L. Vega-Loyo, S.A. Tomás, G.F. Goya and J. Santoyo-Salazar. Direct polyphenol attachment on the surfaces of magnetite nanoparticles, using *Vitis vinifera*, *Vaccinium corymbosum*, or *Punica granatum*. *Nanomaterials* 2023, **13**, 2450.

56. M. Pavlicevic, L. Pagano, M. Villani, A. Zappettini, L. Paesano, U. Bonas, N. Marmiroli and M. Marmiroli. Comparison of Effect of CdS QD and ZnS QD and Their Corresponding Salts on Growth, Chlorophyll Content and Antioxidative Capacity of Tomato. *Int J Phytoremediation.* 2024, **26(6)**, 850-861.

57. A. Barbasz, B. Kreczmer and M. Oćwieja. How the surface properties affect the nanocytotoxicity of silver? Study of the influence of three types of nanosilver on two wheat varieties. *Acta Physiol Plant*., 2018, **40**, 31.

58. M. Hasanuzzaman, K. Nahar, T.I. Anee and M. Fujita. Glutathione in plants: biosynthesis and physiological role in environmental stress tolerance. *Physiol Mol Biol Plants*. 2017, **23(2),** 249-268.

59. M. Carreon-Gonzalez and J.R. Alvarez-Idaboy. The Synergy between glutathione and phenols-phenolic antioxidants repair glutathione: closing the virtuous circle-a theoretical insight. *Antioxidants (Basel).* 2023, **12(5),** 1125.

60. F. Caruso, S. Incerpi, J. Pedersen, S. Belli, S. Kaur and M. Rossi. Aromatic polyphenol π-π Interactions with superoxide radicals contribute to radical scavenging and can make polyphenols mimic superoxide dismutase activity. *Curr Issues Mol Biol.* 2022, 44(11),5209-5220.

61. P. Rai, S. Sharma, S. Tripathi, V. Prakash, K. Tiwari, S. Suri and S. Shivesh. Nanoiron: Uptake, translocation and accumulation in plant systems. *Plant Nano Biol.* 2022, **2**, 100017.

62. H. Tombuloglu, Y. Slimani, S. Akhtar, M. Alsaeed, G. Tombuloglu, M. A. Almessiere, M. S. Toprak, H. Sozeri, A. Baykal and I. Ercan. The size of iron oxide nanoparticles determines their translocation and effects on iron and mineral nutrition of pumpkin (*Cucurbita maxima* L.). *J. Magn. Magn. Mater.* 2022, **564(1)**, 170058.

63. X. Wang, H. Xie, P. Wang and H. Yin. Nanoparticles in plants: uptake, transport and physiological activity in leaf and root. *Materials (Basel)*. 2023, **16(8),** 3097.

64. N. Martineau, J.E. McLean, C.O. Dimkpa, D.W. Britt, A.J. Anderson. Components from wheat roots modify the bioactivity of ZnO and CuO NPs in a soil bacterium. Environ. Pollut. 2014, 187, 65-72.

DATA AVAILABILITY STATEMENT

Data for this article are available at Open Science Framework at https://osf.io/sncmq/